

GSK6853, a Chemical Probe for Inhibition of the BRPF1 Bromodomain

Paul Bamborough,^{||} Heather A. Barnett,[§] Isabelle Becher,[⊥] Mark J. Bird,[§] Chun-wa Chung,^{||} Peter D. Craggs,^{||} Emmanuel H. Demont,^{*,†} Hawa Diallo,[†] David J. Fallon,^{†,#} Laurie J. Gordon,^{||} Paola Grandi,[⊥] Clare I. Hobbs,^{||} Edward Hooper-Greenhill,[‡] Emma J. Jones,^{||} Robert P. Law,^{†,#} Armelle Le Gall,^{*,||} David Lugo,[‡] Anne-Marie Michon,[⊥] Darren J. Mitchell,[†] Rab K. Prinjha,[†] Robert J. Sheppard,^{*,†} Allan J. B. Watson,[#] and Robert J. Watson[†]

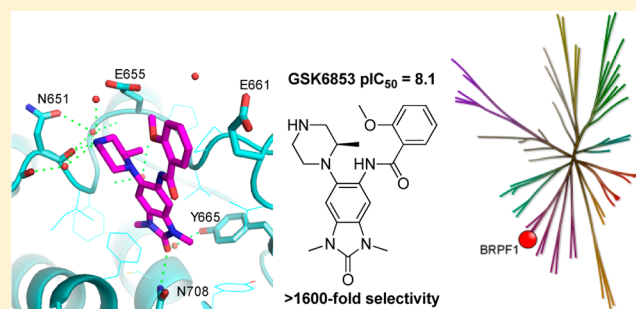
[†]Epinova Discovery Performance Unit, [‡]Quantitative Pharmacology, Experimental Medicine Unit, [§]Flexible Discovery Unit, and ^{||}Platform Technology and Science, GlaxoSmithKline, Gunnels Wood Road, Stevenage, Hertfordshire SG1 2NY, U.K.

[⊥]Cellzome GmbH, GlaxoSmithKline, Meyerhofstrasse 1, 69117 Heidelberg, Germany

[#]WestCHEM, Department of Pure and Applied Chemistry, University of Strathclyde, Thomas Graham Building, 295 Cathedral Street, Glasgow G1 1XL, U.K.

Supporting Information

ABSTRACT: The BRPF (Bromodomain and PHD Finger-containing) protein family are important scaffolding proteins for assembly of MYST histone acetyltransferase complexes. A selective benzimidazolone BRPF1 inhibitor showing micromolar activity in a cellular target engagement assay was recently described. Herein, we report the optimization of this series leading to the identification of a superior BRPF1 inhibitor suitable for *in vivo* studies.



KEYWORDS: BRPF1, BRPF2, BRD1, BRPF3, BET, bromodomain, epigenetics, chemical probe, inhibitor

There are at least 56 bromodomain modules contained within 42 human chromatin-regulator proteins.¹ Of these, the eight bromodomains of the BET (Bromodomain and Extra Terminal) subfamily (BRD2/3/4/T) have received most attention following the discovery that small-molecule inhibitors found during cellular screening campaigns bind to these targets and act by blocking their binding to *N*-acetyl-lysine (KAc) modified histones.^{2–5} Inhibitors of BET proteins, such as I-BET762, RVX-208, OTX-015, and CPI-0610, have progressed into clinical evaluation for oncology and cardiovascular disease.^{6,7}

The phenotypic effects of inhibiting other bromodomains remain to be discovered. The dearth of potent inhibitors of these bromodomains is one factor, but the problem is exacerbated by the significant and diverse phenotypic responses associated with inhibition of the BET proteins.⁸ These can complicate the interpretation of phenotypic readouts obtained with poorly selective inhibitors. Biological evidence links several non-BET bromodomain-containing proteins to disease,⁹ but because of the multidomain architecture and scaffolding function of these proteins the precise role of the bromodomain is often uncertain. For example, the BRPF (Bromodomain and PHD Finger-containing) family of BRPF1, BRPF2/BRD1, and BRPF3 (Figure S1, Supporting Information) act to facilitate the

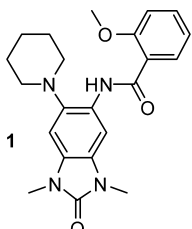
assembly of MYST-family histone acetyltransferase complexes.^{10,11} In addition to the bromodomain, which binds acetylated histones,¹² the proteins contain other histone-binding domains (PZP and PWWP).^{13–15} The availability of potent and selective chemical probes for BRPF bromodomains would significantly enhance our ability to dissect their biological role and better understand the therapeutic opportunities.

We recently reported the discovery of the BRPF1 bromodomain inhibitor **1** (GSK5959) (Table 1).¹⁷ In the BROMOscan panel of 34 bromodomain binding assays, it showed 10 nM BRPF1 inhibition, 90-fold selectivity over BRPF2, and over 500-fold selectivity over all members of the BET family. Others have independently found related BRPF1 inhibitors with similar properties.¹⁸ Although the qualities of **1** made it an excellent probe to further elucidate the role of the BRPF1 bromodomain in many situations, its physicochemical properties and solubility are suboptimal. As part of our ongoing efforts to develop bromodomain probe molecules we sought to obtain an inhibitor with lower logD, solubility >100 μg/mL, and cellular activity < 100 nM.

Received: March 2, 2016

Accepted: May 9, 2016

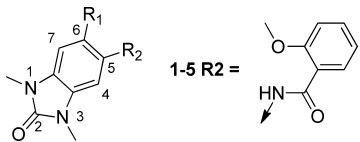
Published: May 9, 2016

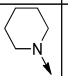
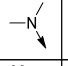

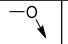
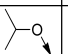
Table 1. Summary of the Properties of GSK5959^a


BRPF1	TR-FRET pIC ₅₀	7.1
	BROMOscan pK _d	8.0
	NanoBRET pIC ₅₀	6.0
BRPF 2/3	TR-FRET pIC ₅₀	5.2/4.5
BRD4 BD1/2	TR-FRET pIC ₅₀	<4.3/<4.3 ^a
Selectivity	BROMOscan	>90-fold
Chrom logD _{pH 7.4} ¹⁶		6.0
CLND solubility (μg/mL)		8

^aSee also Table S1, Supporting Information.

Expansion of the SAR was carried out via analogue searches within the GSK collection, and bespoke syntheses (Scheme S1). The piperidine of **1** could be truncated to deliver the more potent and ligand efficient inhibitor **2**, albeit at the expense of increased inhibition of BRD4 BD1 (Table 2). Further reduction

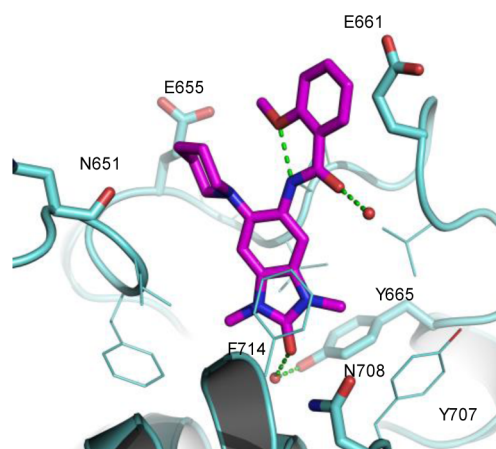
Table 2. SAR at the Benzimidazolone 6-Position^a


R1	#	BRPF1 pIC ₅₀	LE	Chrom logD _{pH7.4}	Solubility ^b	BRD4 BD1 pIC ₅₀
	1	7.1	0.34	6.0	8	< 4.3 ^a
	2	7.3	0.38	4.6	115	5.0
	3	5.8	0.33	3.9	110	<4.3
	4	6.9	0.38	4.1	11	5.0 ^a
	5	7.5	0.38	5.0	9	< 4.3 ^a

^aSee also Table S1, Supporting Information. ^bCLND (μg/mL).

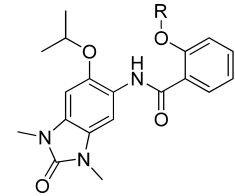
in the size of the 6-substituent (**3**) was detrimental. However, with the ether-linked analogues an increase in potency and selectivity was observed on moving from 6-methoxy **4** to isopropoxy **5**, while ligand efficiency (LE)¹⁹ was retained. Although the discovery of **5** represented a step toward an improved probe in terms of potency, LE, and logD, solubility still remained to be addressed.

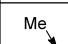
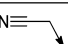
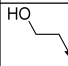
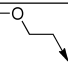
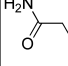
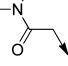
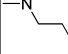
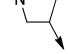
The X-ray complex of BRPF1 with **1** (Figure 1)¹⁷ suggested that the 3- and 4-positions on the benzamide provided vectors suitable for projecting a solubilizing group directly out into solvent, but presented no prospect of gaining interactions with the protein. In contrast, elaboration of the phenyl 2-methoxy also offered the potential to interact with residues of the ZA loop, such as Glu655, while retaining the intramolecular hydrogen-bond seen between the 2-methoxy and the amide

Figure 1. X-ray structure of BRPF1 with **1** (PDB 4UYE).

NH of **1**. Compounds **6–12** were accessed via amide coupling of the appropriate benzoic acids with the aromatic amine (Scheme S1).

While introduction of these groups generally improved solubility relative to **5**, they all resulted in weaker inhibition of BRPF1 (Table 3). This observation was particularly disappoint-

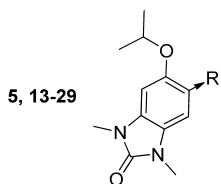
Table 3. Benzamide *ortho*-Position SAR^a


R	#	BRPF1 pIC ₅₀	Solubility ^b	R	#	BRPF1 pIC ₅₀	Solubility ^b
	5	7.5	9		9	6.8	3
	6	6.9	156		10	7.0	174
	7	7.0	19		11	7.0	163
	8	6.5	164		12	6.5	187

^aSee also Table S1, Supporting Information. ^bCLND (μg/mL).

ing for side-chains containing hydrogen-bond donors (**6** and **7**), which were no more potent than close analogues without this functionality (**10**, **11**), hydrogen bond acceptors (**9**), or basic groups (**8** and **12**). These results suggest that introduction of substituents larger than a methyl may give rise to steric clashes with the residues of the ZA loop and suboptimal binding conformations.

With the goals of expanding the diversity of substituents on the 5-position of the benzimidazolone core, improving solubility by lowering logD, and exploring alternatives to the intramolecular methoxy/amide hydrogen-bond, further 5-position analogues were synthesized (Schemes S1 and S2; Table 4). All substituents showed improved solubility relative to **5**, but aliphatic groups, whether linear (**14** and **15**) or cyclic

Table 4. Modifications at the 5-Position^a

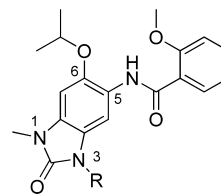
R	#	BRPF1 pIC ₅₀	BRD4 BD1 pIC ₅₀	Sol ^b	R	#	BRPF1 pIC ₅₀	BRD4 BD1 pIC ₅₀	Sol ^b
H	13	5.8	4.4 ^a	114		19	7.2	5.0	126
	14	6.0	<4.3	123		20	5.9	<4.3	154
	15	5.9	<4.3	145		21	6.1	<4.3	157
	16	6.1	<4.3	135		22	6.9	4.6	82
	17	5.8	<4.3	141		23	7.5	5.1	130
	18	6.3	<4.3	164		24	7.0	4.4 ^a	167
	5	7.5	<4.3	9		25	5.7	<4.3	167

^aSee also Table S1, Supporting Information. ^bCLND (μg/mL).

(16 and 17) and positively charged (16) or neutral (14–15, 17) had little effect on potency relative to the 5-H (13) and were over 10-fold less potent than the 2-methoxybenzamide 5.

Consistent with our previous observations for a 6-piperidine,¹⁷ the unsubstituted benzamide 18 is also weaker than the 2-methoxy analogue 5. Presumably this is because the unsubstituted phenyl of 18 is unable to form the intramolecular hydrogen bond with the amide N–H. Anticipating that a 2-pyridyl could mimic this aspect of the 2-methoxy substituent, 19 was synthesized and shown to reduce logD relative to 5 while maintaining potency. The other pyridyl isomers (20 and 21) had activity comparable to the phenyl 18. We interpret this data as supporting the hypothesis that the intramolecular hydrogen bond plays an important role in restricting the degrees of freedom and increasing binding affinity (Figure S2). Further evidence came from the observation that the activities of compounds possessing a 2-heteroatom or 2-OMe group (22–23) retain higher potency than those without. Incorporation of a 6-N into the phenyl ring of 5 is detrimental to activity (compare 24 to 5), probably as a result of electrostatic repulsion between the lone pair of the pyridyl nitrogen and the amide carbonyl. This effect would be greater with the 6-OMe (25), explaining the further drop in potency.

The compounds in Table 4 all met the objective for increased solubility relative to 5. However, it was disappointing that the best balance between BRPF1 potency and selectivity over BRD4 BD1 was achieved with the poorly soluble 2-methoxyphenyl 5. Unable to improve upon the 2-methoxybenzamide in the 5-position, we switched our efforts to the benzimidazolone core itself. Inspection of the structure of 1 bound to BRPF1 (Figure 1) suggested it may be possible for a chain possessing a solubilizing group to pass through the channel between Phe714, Asn708, and Tyr707, although the space for such a group was very limited. Extension of the 3-Me to a hydroxyethyl (Scheme S3) (26) gave a substantial increase in solubility, but with an unacceptable 40-fold drop in BRPF1 inhibition (Table 5).

Table 5. Modifications at the N3-Position^a

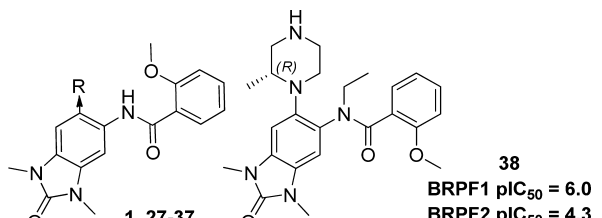
R	#	BRPF1 pIC ₅₀	Solubility (μg/mL)
Me	5	7.5	9
	26	5.9	187

^aSee also Table S1, Supporting Information.

As the 3- and 5-positions seemed unproductive we returned to the 6-position of the benzimidazolone. The crystal structure of 1 in complex with BRPF1 (Figure 1) showed the proximity of the backbone carbonyl of Asn651 to the C4 carbon of the piperidine. It was postulated that introduction of a basic nitrogen in this position could pick up an additional hydrogen bond to this carbonyl, while also improving solubility.

To test this hypothesis, compounds 28–31 were synthesized via S_NAr reaction or Suzuki chemistry on an appropriately substituted core (Schemes S4 and S5). The piperazine 28 was well tolerated, delivering the desired improvement in physicochemical properties while maintaining potency at BRPF1 (Table 6). Methylation of the piperazine to give 4-methylpiperazine 29 was slightly detrimental. The C-linked piperidine 30 and 1,2,3,6-tetrahydropyridine 31, however, were significantly less potent, with the sp³ hybridized carbon being more deleterious than the sp². This is in accordance with our previous observation that the 6-H and 6-Me (3) analogues were ~10-fold less active than the 6-OMe (4). Collectively, the results for compounds 1–5, 28, and 30–31 rule out steric demands as the explanation for the reduced inhibition of carbon-linked 6-substituents. Instead, they provide support for the hypothesis put forward in our previous paper that linking via a heteroatom plays an important role by electrostatically influencing the conformation of the 5-benzamide.¹⁷ This is further supported by the distribution of torsion angles and distances in an analysis of small molecule X-ray structures (Figure S3).

Despite the 40-fold variation in the BRPF1 activities of analogues 1 and 27–31, there was comparatively little change in potency versus the closely related BRPF2 bromodomain

Table 6. Modifications at the 6-Position^a


R	#	pIC ₅₀			Sol ^b	R	#	pIC ₅₀			Sol ^b
		BRPF1	BRD4	BD1				BRPF1	BRD4	BD1	
	27	7.3	<4.3	72		1	7.1	<4.3	8		
	28	7.1	<4.3	135		29	6.7	<4.3	149		
	30	5.5	<4.3	107		31	5.9	<4.3	110		
	32	8.3	5.0	4		33	7.8	4.9	3		
	34	8.1	4.7	140		35	6.9	<4.3	134		
	36	7.1	<4.3	141		37	6.9	4.7	139		

^aSee also Table S1, Supporting Information. ^bCLND ($\mu\text{g/mL}$).

(Table S1). The largest selectivity window over BRPF2 is therefore approximately 160-fold (27 and 28).

Having achieved with 28 acceptable solubility, while maintaining significant BRPF1 inhibition, we next sought to investigate whether improved potency and selectivity was readily achievable. Interrogating the crystal structure of 1 in complex with BRPF1, it was intriguing to note that the 2-position of the piperidine presented a vector toward Pro658 (Figure 2A). This residue is one of the few that are not conserved across the BRPF subfamily, being substituted for Ser592 in BRPF2 or Asn619 in BRPF3. Analysis of the BRPF1 site using GRID probes suggested the potential for favorable interaction with a methyl group in the small indentation in the surface near Pro658 (Figure 2A).²⁰

This hypothesis was first explored with the 2-methyl piperidines 32 and 33. Indeed, a significant increase in BRPF1 inhibition was observed, especially with the (R)-enantiomer, with minimal effect on the inhibition of BRPF2 (Table S1, compare 32 with 27), BRPF3, and BRD4 (Table 6). Transferring these findings to the more soluble piperazines (34–35) again showed the (R)-enantiomer 34 to be the most potent. The comparatively weaker inhibition with the 2-(S)-enantiomer 35, and 3-methyl enantiomers (36–37), confirm the specificity of this interaction.

Shortly afterward a 2.0 Å crystal structure of the BRPF1 bromodomain in complex with 34 was obtained (Figure 2B). This showed that 34 binds to BRPF1 in a very similar way to 1. As expected, the 2-methylpiperidine occupies the pocket close to Pro658, and the piperazine 4-NH makes a direct hydrogen bond to the backbone carbonyl of Asn651. Overlaying the apo structure of BRPF2 highlights the structural differences

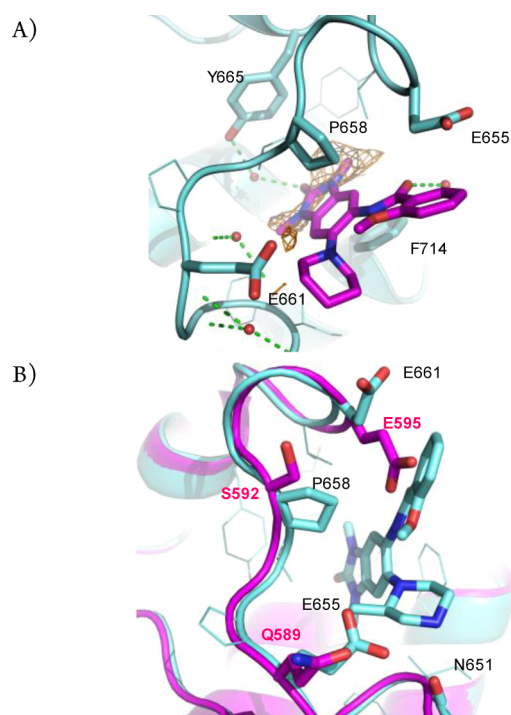


Figure 2. (A) GRID map analysis using the BRPF1 structure of compound 1 (PDB 4UYE). Methyl probe is shown in orange mesh. (B). X-ray structure of BRPF1 (cyan, PDB 5G4R) with 34, overlaid with BRPF2 apo (magenta, PDB 3RCW).

between the isoforms, which the 2-methyl substituent is able to exploit.

To facilitate interpretation of phenotypic assays we designed a less active analogue of 34 in which the 5-amide was alkylated, 38 (Scheme S5, GSK9311). We reasoned that this would prevent the 5-aryl group from adopting the conformation observed in the structures of 1 and 34 because of the loss of all internal hydrogen-bonding interactions, and steric clashes between the amide N-alkyl group and both the piperazine and the *o*-methoxy substituents. Usefully, this change resulted in a 100-fold drop in BRPF1 inhibition. This result can be rationalized by a crystal structure of 38 in BRPF1 in which the benzamide group packs poorly against P658 and E661 (Figure 3).

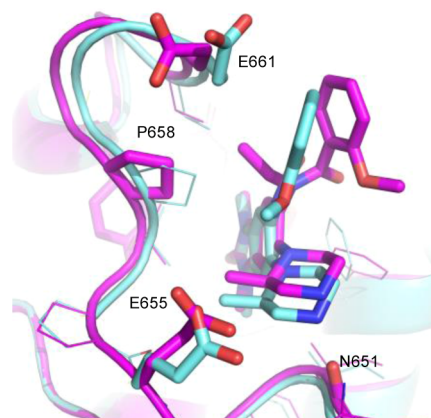


Figure 3. X-ray structures of BRPF1 with 34 (cyan, PDB 5G4R) and 38 (magenta, PDB 5G4S).

Compound **34** was tested in the BROMOscan panel of bromodomain binding assays (DiscoverX). Consistent with the data above, it showed excellent BRPF1 potency (pK_d 9.5) and greater than 1600-fold selectivity over all other bromodomains tested (Table S2). To our knowledge this is the most potent and selective inhibitor of any single bromodomain reported to date.

All biochemical data presented thus far was determined using recombinant, truncated bromodomains. Potent binding to full-length endogenous BRPF1 (pIC_{50} 8.6) was confirmed in a chemoproteomic competition binding assay using pull-down of lysate from HuT-78 cells followed by immuno readout (Figure 4). Selectivity over endogenous BRD3 was also shown.

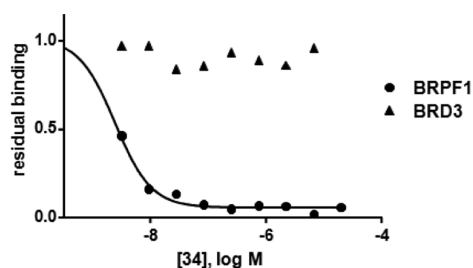


Figure 4. Potency for endogenous cellular BRPF1. pIC_{50} of **34** for BRPF1 and BRD3 measured in a chemoproteomic competition binding assay (Supplementary Methods, Supporting Information).

Compounds **34** and **38** were assessed in a cellular protein interaction assay measuring the displacement of NanoLuc-tagged BRPF1 bromodomain from Halo-tagged histone H3.3 to demonstrate cell permeability and disruption of chromatin binding (Supplementary Methods, Supporting Information).²¹ Compound **34** exhibited potent inhibition (Figure S7) with pIC_{50} 7.7, a 50-fold improvement over **1**. The less active analogue **38** gave a reduced effect (pIC_{50} 5.4), in line with its biochemical data.

Screening **34** against a panel of 48 unrelated assays revealed only off-target activities that are relatively weak compared to the BRPF1 potency (Table S3). However, to minimize the chance of off-target effects we recommend that a concentration of no higher than 1 μ M should be used in cell-based assays. To assess the suitability of compound **34** for *in vivo* studies, its DMPK characteristics were determined in male CD1 mice via *iv*, *po*, and *ip* administration. The results indicate that the *ip* route of administration would be suitable for dosing this molecule in potential PK/PD models. In order to be able to compare biochemical potency measurements to free blood concentrations, the fraction unbound (f_{ub}) in the CD1 mouse was also determined with a resulting value of 7.9% (Table 7 and Table S4).

To conclude, we have optimized compound **1** to produce **34** (GSK6853), a potent (300 pM), soluble, cell active (20 nM), and highly selective inhibitor of the BRPF1 bromodomain, and demonstrated properties suitable for cellular and *in vivo* studies. We hope that disclosure of this chemical probe will stimulate further investigation into the functions of the BRPF1 bromodomain.

Table 7. Summary of Properties of Compound 34^a

BRPF1	TR-FRET pIC_{50}	8.1
	BROMOscan pK_d	9.5
	NanoBRET pIC_{50} ^b	7.7
BRPF 2/3	TR-FRET pIC_{50}	5.1/4.8
BRD4 BD1/2	TR-FRET pIC_{50}	4.7 ^c / $<$ 4.3
selectivity ^c	BROMOscan	$>$ 1600-fold
Chrom $\log D_{pH\ 7.4}$ ¹⁶		2.0
CLND solubility (μ g/mL)		140
<i>iv</i> CLb (mL/min/kg)/ $t_{1/2}$ (h)		107/1.7
F% <i>ip/po</i> (3 mg/kg)		85/22

^aSee also Table S1, Supporting Information. ^bPromega Corp., Figure S5. ^cDiscoverX Corp., Table S2.

■ ASSOCIATED CONTENT

📄 Supporting Information

The Supporting Information is available free of charge on the ACS Publications website at DOI: 10.1021/acsmchemlett.6b00092.

Synthetic procedures, analytical data, methods, Figures S1–S7, and Tables S1–S3 (PDF)

■ AUTHOR INFORMATION

Corresponding Authors

*E-mail: emmanuel.h.demont@gsk.com.

*E-mail: armelle.5.le-gall@gsk.com.

*E-mail: Robert.Sheppard@astrazeneca.com.

Present Addresses

(R.J.S.) Oncology Innovative Medicines and Early Development, AstraZeneca, Cambridge Science Park, Milton Road, Cambridge CB4 0WG, U.K.

(I.B.) Genome Biology Unit, European Molecular Biology Laboratory, Meyerhofstrasse 1, Heidelberg, Germany.

Notes

The authors declare no competing financial interest.

Biographies

Armelle Le Gall gained her MSc in Chemoinformatics from the University of Sheffield, U.K. After graduating, she joined GSK, where she is currently an Investigator in the Molecular Design department. She has been mainly involved in medicinal chemistry projects in the Respiratory and Immuno-Inflammation Therapeutic areas. Most recently, her research has focused on structure-based drug design, in particular, including protein flexibility, and also high throughput screening data analysis.

Robert J. Sheppard graduated with a degree in Chemistry from the University of Oxford in 1997. After joining SmithKline Beecham he worked on the design and synthesis of novel antibacterial agents targeting tRNA synthetases, bacterial topoisomerase, and the ribosome. In 2009 he moved to GSK's Epinova Discovery Performance Unit as a team leader focussed on developing inhibitors of epigenetic proteins including demethylases, deiminases, and bromodomains. Robert moved to AstraZeneca's Oncology iMED in 2015 where he maintains a strong interest in the role of epigenetics in cancer and immuno-oncology. He represents AstraZeneca in the Kinetics for Drug Discovery Innovative Medicines Initiative.

■ ACKNOWLEDGMENTS

We thank Jacqui Méndez and Danette Daniels of Promega Corporation for facilitating NanoBRET assays. Thanks to Tony Cooper for chemistry and discussion, Eric Hortense and Steve

Jackson for chiral separations, Douglas Minick for vibrational CD, Richard Upton for NMR, Nicholas Leach and Fiona Shilliday for crystallization, and Melanie Leveridge for help with manuscript preparation. All animal studies were ethically reviewed and carried out in accordance with Animals (Scientific Procedures) Act 1986 and the GSK Policy on the Care, Welfare and Treatment of Animals.

ABBREVIATIONS

CLND, ChemiLuminescent Nitrogen Detection; LE, ligand efficiency; KAc, acetyl-lysine; Sol, solubility

REFERENCES

- (1) Filippakopoulos, P.; Picaud, S.; Mangos, M.; Keates, T.; Lambert, J. P.; Barsyte-Lovejoy, D.; Felletar, I.; Volkmer, R.; Muller, S.; Pawson, T.; Gingras, A. C.; Arrowsmith, C. H.; Knapp, S. Histone recognition and large-scale structural analysis of the human bromodomain family. *Cell* **2012**, *149*, 214–231.
- (2) Nicodeme, E.; Jeffrey, K. L.; Schaefer, U.; Beinke, S.; Dewell, S.; Chung, C. W.; Chandwani, R.; Marazzi, L.; Wilson, P.; Coste, H.; White, J.; Kirilovsky, J.; Rice, C. M.; Lora, J. M.; Prinjha, R. K.; Lee, K.; Tarakhovskiy, A. Suppression of inflammation by a synthetic histone mimic. *Nature* **2010**, *468*, 1119–1123.
- (3) Filippakopoulos, P.; Qi, J.; Picaud, S.; Shen, Y.; Smith, W. B.; Fedorov, O.; Morse, E. M.; Keates, T.; Hickman, T. T.; Felletar, I.; Philpott, M.; Munro, S.; McKeown, M. R.; Wang, Y.; Christie, A. L.; West, N.; Cameron, M. J.; Schwartz, B.; Heightman, T. D.; La, T. N.; French, C. A.; Wiest, O.; Kung, A. L.; Knapp, S.; Bradner, J. E. Selective inhibition of BET bromodomains. *Nature* **2010**, *468*, 1067–1073.
- (4) Chung, C.; Coste, H.; White, J. H.; Mirguet, O.; Wilde, J.; Gosmini, R. L.; Delves, C.; Magny, S. M.; Woodward, R.; Hughes, S. A.; Boursier, E. V.; Flynn, H.; Bouillot, A. M.; Bamborough, P.; Brusq, J. M.; Gellibert, F. J.; Jones, E. J.; Riou, A. M.; Homes, P.; Martin, S. L.; Uings, I. J.; Toum, J.; Clement, C. A.; Boullay, A. B.; Grimley, R. L.; Blandel, F. M.; Prinjha, R. K.; Lee, K.; Kirilovsky, J.; Nicodeme, E. Discovery and Characterization of Small Molecule Inhibitors of the BET Family Bromodomains. *J. Med. Chem.* **2011**, *54*, 3827–3838.
- (5) Garnier, J. M.; Sharp, P. P.; Burns, C. J. BET bromodomain inhibitors: a patent review. *Expert Opin. Ther. Pat.* **2014**, *24*, 185–199.
- (6) Mirguet, O.; Gosmini, R.; Toum, J.; Clement, C. A.; Barnathan, M.; Brusq, J.; Mordaunt, J. E.; Grimes, R. M.; Crowe, M.; Pineau, O.; Ajakane, M.; Daugan, A.; Jeffrey, P.; Cutler, L.; Haynes, A. C.; Smithers, N. N.; Chung, C.; Bamborough, P.; Uings, I. J.; Lewis, A.; Witherington, J.; Parr, N.; Prinjha, R. K.; Nicodeme, E. Discovery of epigenetic regulator I-BET762: Lead optimization to afford a clinical candidate inhibitor of the BET bromodomains. *J. Med. Chem.* **2013**, *56*, 7501–7515.
- (7) Filippakopoulos, P.; Knapp, S. Targeting bromodomains: epigenetic readers of lysine acetylation. *Nat. Rev. Drug Discovery* **2014**, *13*, 337–356.
- (8) Muller, S.; Knapp, S. Discovery of BET bromodomain inhibitors and their role in target validation. *MedChemComm* **2014**, *5*, 288–296.
- (9) Chung, C.; Tough, D. Bromodomains: a new target class for small molecule drug discovery. *Drug Discovery Today: Ther. Strategies* **2012**, *9*, e111–e120.
- (10) Carlson, S.; Glass, K. C. The MOZ Histone Acetyltransferase in Epigenetic Signaling and Disease. *J. Cell. Physiol.* **2014**, *229*, 1571–1574.
- (11) Ullah, M.; Pelletier, N.; Xiao, L.; Zhao, S. P.; Wang, K.; Degerny, C.; Tahmasebi, S.; Cayrou, C.; Doyon, Y.; Goh, S. L.; Champagne, N.; Cote, J.; Yang, X. J. Molecular architecture of quartet MOZ/MORF histone acetyltransferase complexes. *Mol. Cell. Biol.* **2008**, *28*, 6828–6843.
- (12) Poplawski, A.; Hu, K.; Lee, W.; Nateson, S.; Peng, D.; Carlson, S.; Shi, X.; Balaz, S.; Markley, J. L.; Glass, K. C. Molecular insights into recognition of N-terminal histone modifications by the BRPF1 bromodomain. *J. Mol. Biol.* **2014**, *426*, 1661–1676.
- (13) Qin, S.; Jin, L.; Zhang, J.; Liu, L.; Ji, P.; Wu, M.; Wu, J.; Shi, Y. Recognition of unmodified histone H3 by the first PHD finger of bromodomain-PHD finger protein 2 provides insights into the regulation of histone acetyltransferases monocytic leukemic zinc-finger protein (MOZ) and MOZ-related factor (MORF). *J. Biol. Chem.* **2011**, *286*, 36944–36955.
- (14) Laue, K.; Daujat, S.; Crump, J. G.; Plaster, N.; Roehl, H. H.; Kimmel, C. B.; Schneider, R.; Hammerschmidt, M. The multidomain protein BRPF1 binds histones and is required for Hox gene expression and segmental identity. *Development* **2008**, *135*, 1935–1946.
- (15) Vezzoli, A.; Bonadies, N.; Allen, M. D.; Freund, S. M.; Santiveri, C. M.; Kvinlaug, B. T.; Huntly, B. J.; Gottgens, B.; Bycroft, M. Molecular basis of histone H3K36me₃ recognition by the PWWP domain of Brpf1. *Nat. Struct. Mol. Biol.* **2010**, *17*, 617–619.
- (16) Young, R. J.; Green, D. V. S.; Luscombe, C. N.; Hill, A. P. getting physical in drug discovery II: the impact of chromatographic hydrophobicity measurements and aromaticity. *Drug Discovery Today* **2011**, *16*, 822–830.
- (17) Demont, E. H.; Bamborough, P.; Chung, C.; Craggs, P. D.; Fallon, D.; Gordon, L. J.; Grandi, P.; Hobbs, C. I.; Hussain, J.; Jones, E. J.; Le Gall, A.; Michon, A.; Mitchell, D. J.; Prinjha, R. K.; Roberts, A. D.; Sheppard, R. J.; Watson, R. J. 1,3-Dimethyl Benzimidazolones are potent, selective inhibitors of the BRPF1 bromodomain. *ACS Med. Chem. Lett.* **2014**, *5*, 1190–1195.
- (18) (a) Palmer, W. S.; Poncet-Montange, G.; Liu, G.; Petrocchi, A.; Reyna, M.; Subramanian, G.; Theroff, J.; Yau, A.; Kost-Alimova, M.; Bardenhagen, J. P.; Leo, E.; Shepard, H. E.; Tieu, T. N.; Shi, X.; Zhan, Y.; Zhao, S.; Draetta, G.; Toniatti, C.; Jones, P.; Do, M. G.; Andersen, J. N. Structure-guided design of IACS-9571, a selective high-affinity dual TRIM24-BRPF1 bromodomain inhibitor. *J. Med. Chem.* **2016**, *59*, 1440–1454. (b) Bennett, J.; Fedorov, O.; Tallant, C.; Monteiro, O.; Meier, J.; Gamble, V.; Savitsky, P.; Nunez-Alonso, G. A.; Haendler, B.; Rogers, C.; Brennan, P. E.; Muller, S.; Knapp, S. Discovery of a chemical tool inhibitor targeting the bromodomains of TRIM24 and BRPF1. *J. Med. Chem.* **2016**, *59*, 1642–1647. (c) Epigenetics Probes Collection. <http://www.thesgc.org/chemical-probes/epigenetics> (see PFI-4, OF-1, and NI-57).
- (19) (a) Kuntz, I. D.; Chen, K.; Sharp, K. A.; Kollman, P. A. The maximal affinity of ligands. *Proc. Natl. Acad. Sci. U. S. A.* **1999**, *96*, 9997–10002. (b) Hopkins, A. L.; Groom, C. R.; Alex, A. Ligand efficiency: a useful metric for lead selection. *Drug Discovery Today* **2004**, *9*, 430–431.
- (20) Goodford, P. J. A computational procedure for determining energetically favorable binding sites on biologically important macromolecules. *J. Med. Chem.* **1985**, *28*, 849–857.
- (21) Deplus, R.; Delatte, B.; Schwinn, M. K.; Defrance, M.; Mendez, J.; Murphy, N.; Dawson, M. A.; Volkmar, M.; Putmans, P.; Calonne, E.; Shih, A. H.; Levine, R. L.; Bernard, O.; Mercher, T.; Solary, E.; Urh, M.; Daniels, D. L.; Fuks, F. TET2 and TET3 regulate GlcNAcylation and H3K4 methylation through OGT and SET1/COMPASS. *EMBO J.* **2013**, *32*, 645–655.